# Analysis of the Effect of Severe Accident Scenario on the Vessel Lower Head Failure in Nordic BWR using MELCOR code

**Sergey Galushin\* and Pavel Kudinov**
Royal Institute of Technology
Roslagstullsbacken 21, SE-106 91, Stockholm, Sweden
galushin@kth.se, pkudinov@kth.se

**Abstract:** Severe accident management (SAM) in Nordic boiling water reactors (BWR) relies on ex-vessel core debris coolability. In case of core melt and vessel failure, melt is poured into a deep pool of water located under the reactor. The melt is expected to fragment, quench, and form a debris bed, coolable by natural circulation of water. Success of the strategy is contingent upon melt release conditions from the vessel which determine (i) properties and thus coolability of the debris bed, and (ii) potential for energetic steam explosion. Both non-coolable debris bed and steam explosion are credible threats to containment integrity. Melt release conditions are the major source of uncertainty in quantification of the risk of containment failure in Nordic BWRs using ROAAM+ Framework. The melt release conditions, including in-vessel\ex-vessel pressure, lower drywell pool depth and temperature, are affected by aleatory (severe accident scenario) and epistemic (modeling) uncertainties.

In this work we use MELCOR code to perform the analysis of the effects of Severe accident scenarios and modelling options in MELCOR on the properties of debris relocated to the lower head, the time and the mode of vessel lower head failure. We identify the most influential uncertain factors and discuss the needs for improvements in the modeling approaches.

**Keyword:** Severe Accident Nordic BWR MELCOR ROAAM

## 1. INTRODUCTION

Severe accident management in Nordic Boiling Water Reactors (BWR) relies on ex-vessel core debris coolability. In case of core melt and vessel failure, melt is poured into a deep pool of water located under the reactor (lower dry well (LDW)). The melt is expected to fragment, quench, and form a debris bed, coolable by natural circulation of water. Success of the strategy is contingent upon melt release conditions from the vessel which determine (i) properties and thus coolability of the bed, (ii) potential for energetic steam explosions. If decay heat cannot be removed from the debris bed, the debris can re-melt and attack containment basemat. Strong steam explosion can damage containment structures. Melt release conditions are recognized as the major source of uncertainty in quantification of the risk of containment failure in Nordic BWRs [1,2,3].

This work is focused on the evaluation of the effect of severe accident scenario on the time and mode of vessel failure and melt release conditions in Nordic BWR. We use MELCOR 2.1 code for prediction of the in-vessel phase of accident progression, vessel failure and melt release [11,12]. The main goal of this paper is to characterize the range of possible debris properties in lower plenum at the time of the release, melt release conditions (e.g. debris ejection rate, enthalpy release rate) and its sensitivity to accident scenario and MELCOR modelling options of vessel failure (penetration failure vs. vessel wall failure) and melt release (solid debris ejection switch IDEJ), which is of paramount importance for the risk analysis in the ROAAM+ framework.

## 2. APPROCH

In the analysis presented in this paper we consider a severe accident initiated by the station blackout (SBO) scenario with a delayed power recovery. We consider a simultaneous loss of the offsite power (LOOP) and backup diesel generators. This results in the simultaneous loss of all water injection systems, including crud purge flow through the control rod drive tubes. This kind of accident is one of the most challenging accidents scenarios for BWR's as illustrated at Fukushima-Daiichi accident [4] and is among the major contributors to the core damage frequency (CDF) for Nordic BWR according

to PSA Level 1 analysis. We consider that the power (external grid or diesel generators) can be recovered after some time delay and emergency core cooling system (ECCS) system can be restarted. According to the considered scenario, the operator can delay activation of the depressurization system to keep coolant in the vessel. Yet, for injection of water with low pressure ECCS, depressurization has to be activated.

## 2.1. MELCOR model of Nordic BWR

MELCOR input model for Nordic BWR was originally developed for accidents analysis in the power uprated plants [5]. Nordic BWR MELCOR model have total thermal power output of 3900 MW. The core consists of 700 fuel assemblies of SVEA-96 Optima2 type – which is divided into five non-uniform radial rings and eight axial levels. The primary coolant system is represented by 27 control volumes (CV), connected with 45 flow paths (FL) and 73 heat structures (HS). The core and lower plenum is represented by a 6-ring, 19-axial level control volume geometry. In the analysis of the vessel lower head behaviour we consider two options: i) with penetration modelling, i.e. we model one IGT and one CRGT in radial rings 1-5. So the vessel lower head can failure due to penetration failure and/or vessel wall creep rupture; ii) without penetration modelling, vessel lower head failure due to vessel wall creep rupture.

In this work we use MELCOR code version 2.1 (rev7544) [6,7] for prediction of the effect of MELCOR modelling parameters on the in-vessel phase of accident progression, timing and mode of vessel failure and melt release.

*MELCOR Modelling of Vessel Lower Head Failure and Melt Release*

MELCOR Assumes the following mechanisms of RPV Lower Head (LH) breach (not mutually exclusive): (i) Vessel wall failure, which uses creep-rupture model (1D options was used [6,7]). Creep-rupture failure of a lower head segment occurs, in response to mechanical loading under conditions of material weakening at elevated temperatures; (ii) Penetration failure, due to the temperature of a penetration (or the temperature of the innermost node of the lower head) reaches a failure temperature (TPFAIL=1273K was used in the analysis) specified by the user, or a logical control function specified by user [6,7].

Whenever any failure condition is satisfied, an opening with an initial diameter defined by the user is established (either default value of 0.1m, or user-specified values that corresponds to penetrations diameters (e.g IGT – 0.07m, CRGT – 0.14m).

After a failure has occurred, the mass of each material in the bottom axial level that is available for ejection (but not necessarily ejected) is calculated. Two simple options exist (Solid debris ejection switch). In the default option (ON, IDEJ = 0), the masses of each material available for ejection are the total debris and molten pool material masses, regardless of whether or how much they are molten. In the second option (OFF, IDEJ = 1), the masses of steel, Zircaloy, and UO2 available for ejection are simply the masses of these materials that are molten; the masses of steel oxide and control poison materials available for ejection are the masses of each of these materials multiplied by the steel melt fraction, based on an assumption of proportional mixing; the mass of ZrO2 available for ejection is the ZrO2 mass multiplied by the Zircaloy melt fraction. Additionally, the mass of solid UO2 available for ejection is the Zircaloy melt fraction times the mass of UO2 that could be relocated with the Zircaloy as calculated in the candling model using the secondary material transport model [6,7]. Furthermore, MECLOR puts additional constraints on the mass to be ejected at vessel failure: (i) the mass of molten material should be at least C1610(2) value (5000kg – default value, 0kg – was used in the analysis) or a melt fraction of C1610(1) (0.1 – default value, 0 – was used in the analysis) to initiate melt ejection. Additionally, in case of gross failure of vessel wall, it is assumed that all debris in the bottom axial level of the corresponding ring, regardless its state, is discharged linearly over 1s time step without taking into account failure opening diameter [6,7]. The maximum mass of all materials that can be ejected during a single COR package time step is calculated as [6,7]:

$$M_{ej} = \rho_m A_f v_{ej} \Delta t \tag{1}$$

where $\rho_m$ – is density of material being ejected, $A_f$ - failure area, $v_{ej}$ – velocity of debris being ejected, $\Delta t$ – COR package time step. The fraction of the total mass available for ejection that actually is ejected during the subcycle is $M_{ej}$ divided by the total mass available to be ejected, up to a maximum value of 1.0. This fraction is applied to the mass of each material available for ejection [6,7]. The velocity of material being ejected is calculated by:

$$v_{ej} = C_d(2\Delta P/\rho_m + 2g\Delta z_d) \qquad (2)$$

where $C_d$ – is flow discharge coefficient ($C_d = 1$ was used in the analysis presented in this paper), $\Delta P$ – pressure difference between the LP and reactor cavity control volumes, $g$ – gravitational acceleration constant, and $\Delta z_d$ – debris and molten pool height (see references [6,7] for more details).

In the analysis presented in this paper we consider the effect of MELCOR modelling options of vessel failure (i.e. penetration failure vs. vessel wall failure (without penetration modelling)) and the effect of MELCOR modelling of melt release (solid debris ejection switch IDEJ = 0 and 1).

*Sampling of accident scenario parameters*

For the analysis of the effect of severe accident scenario on the process of core degradation and relocation into the LP we employ uniform mesh sampling in the space of scenario parameters. The results of simulations also used for the development of the database of full model solutions [14]. We consider the time delay for activation of the depressurization system - ADS (System 314) to be uniformly distributed in the range from 1000 to 10000 seconds after the initiating event; (ii) the time delay for the activation of low-pressure coolant injection (System 323) is also in the range from 1000 to 10000 seconds after the initiating event, however low-pressure injection can be initiated only after depressurization.

## 3. RESULTS

The analysis of the effect of severe accident scenario (ADS and ECCS Timing) on the process of core degradation, relocation to lower plenum, vessel failure and melt release has been performed using MELCOR 2.1 rev7544. In the analysis we considered different timing of activation of ADS and ECCS (see Section 2). Furthermore, the effect of maximum time step in MELCOR code was also considered in the analysis (6 different values), since it was previously show that MELCOR time step can have quite significant effect on the results and the lack of time step convergence of the solution with the reduction of the maximum time step [14,15,16]. In the analysis presented in this paper we also consider the effect of MELCOR modelling of vessel failure (penetration failure vs. vessel wall failure) and modelling of melt release (solid debris ejection switch IDEJ).

The results presented as two-dimensional maps (120 accident scenarios (ADS – ECCS Timing combinations)), where different figures-of-merit are presented as expected values (as expected value of the results obtained with different time steps, 6 – MELCOR code runs with different max. time step were performed for every accident scenario, 2160 cases were simulated in total) color-coded according to the corresponding colorbar, as functions of accident scenario timings (ADS and ECCS Timing).

Figure 1 show the effect of the accident scenario on the timing of core support plate failure, the results show that the core support failure and debris relocation to the lower plenum can be prevented if ADS is activated within ~4000 sec after initiating event and ECCS is initiated within 1500-2000sec after depressurization. Furthermore, the results show that the failure of core support occurs earlier in scenarios with early depressurization, compared to scenarios with late depressurization (with max. values at ADS time in the range of 4000-6000 sec). After 6000sec after initiating event ADS is ineffective in prevention\delay of the core support plate failure.

Figure 2a illustrate the mass of hydrogen generated in-vessel with penetration modelling, and Figure 2b without penetration modelling. The results show that the amount of hydrogen produced in-vessel is significantly smaller in the scenarios with early depressurization (ADS time below 3500sec) compared to scenarios with late depressurization, which was also illustrated in [18,19]. Furthermore, the results show that the effect of vessel failure modelling (i.e. penetration vs. vessel wall failure) has an effect on the amount of hydrogen produced in-vessel, however it can be considered as insignificant, since the major part of hydrogen is produced during in-core accident progression [18,19].
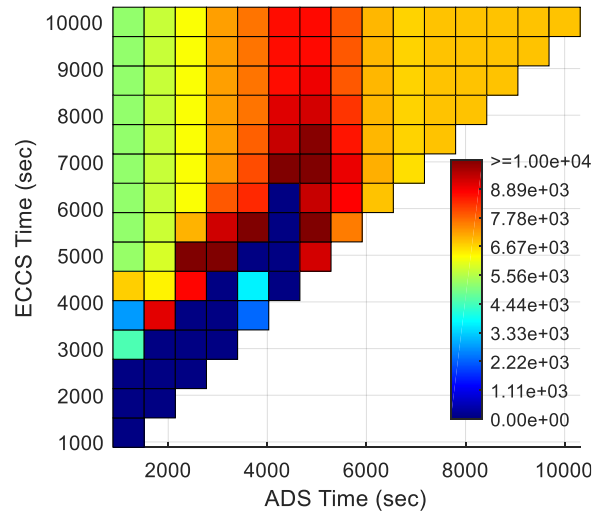
Figure 1. Expected value of the Time of Core Support Plate Failure (sec) as a function of ADS and ECCS Timing (sec)
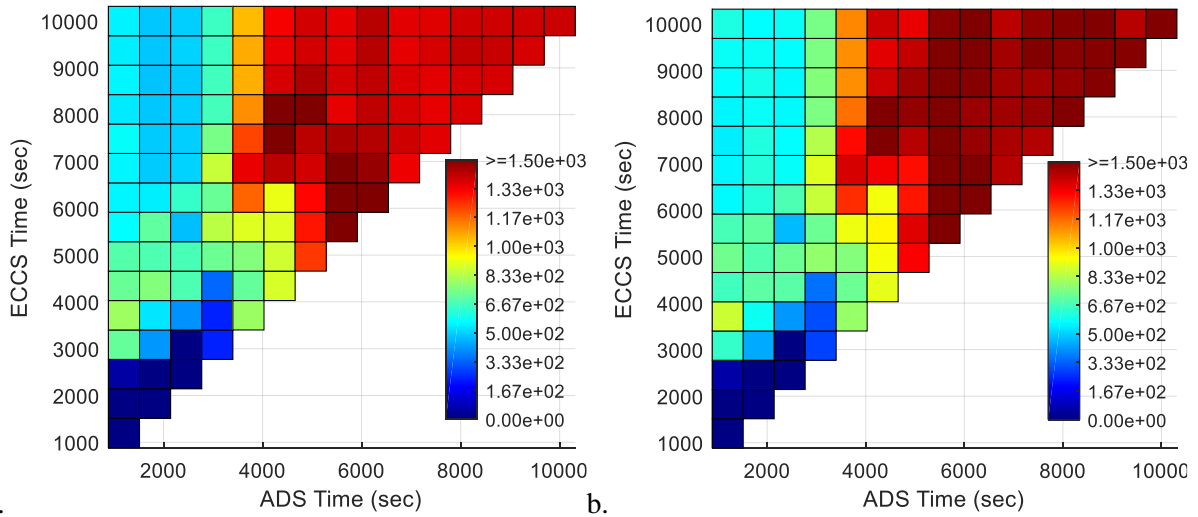


a.

b.

Figure 2. Expected value of the hydrogen mass generated in-vessel before vessel breach (kg) (a) with penetration modelling (b) without penetration modelling; as a function of ADS and ECCS Timing (sec)
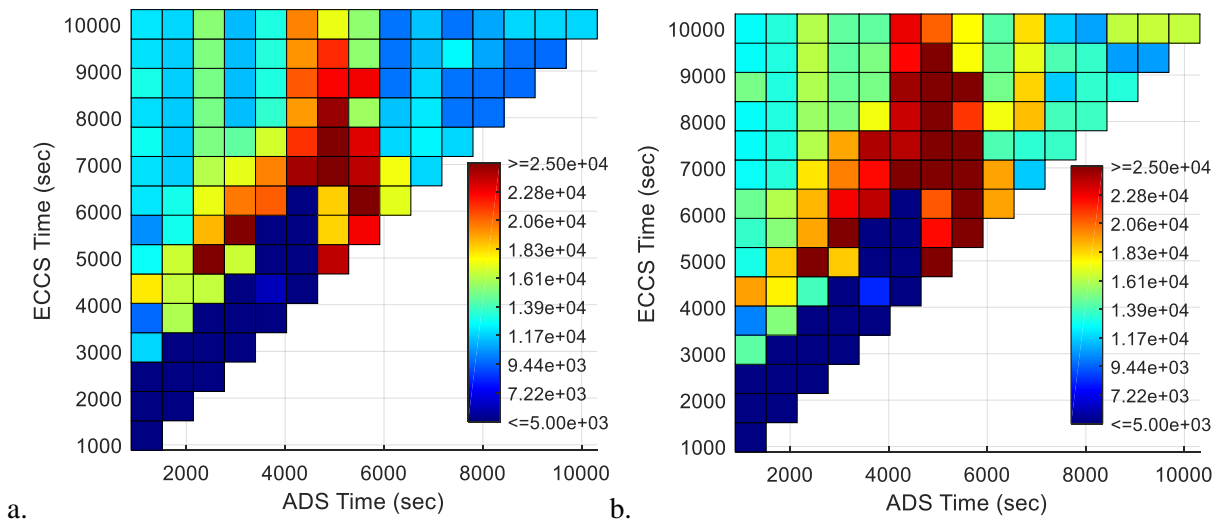


a.

b.

Figure 3. Expected value of (a) time of vessel failure (sec) (b) time of the onset of the release (sec), with penetration modelling; as a function of ADS and ECCS Timing (sec)

Figure 3a present the timing of vessel breach due to penetration failure (with penetration modelling) as a function of accident scenario. The results show that the penetration failure occurs at approximately 10000-15000sec in scenarios with early and late depressurization and late water injection (after 7000sec). Furthermore, apparently there is a domain of scenarios (with ADS timing in the range of 4000-6000sec) where vessel breach due to penetration failure can be delayed significantly. Figure 3b – shows the timing of melt release (melt release initiation, i.e. ejected mass from the vessel is > 0), according to the results, there is some time delay between the vessel breach and initiation of the debris ejection in the case with penetration modelling in MELCOR.
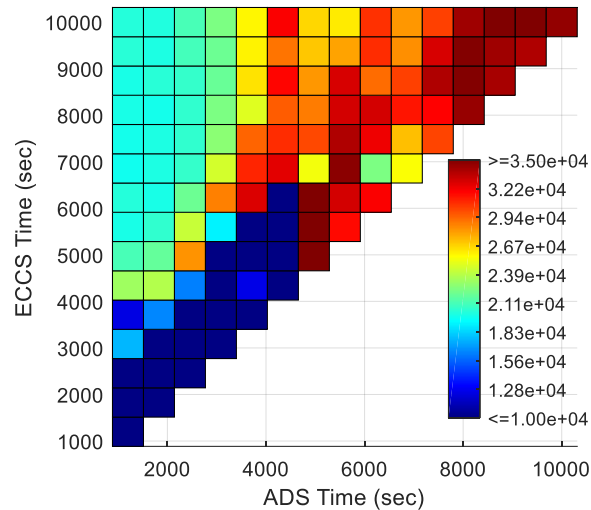


Figure 4. Expected value of the time of vessel failure and the onset of the release (sec), without penetration modelling; as a function of ADS and ECCS Timing (sec)

Figure 4 illustrates the timing of vessel failure and melt release in the case of vessel wall failure (without penetration modelling). The results show that in the scenarios with early depressurization, vessel failure occurs at approximately 20000sec, while in scenarios with late depressurization it occurs after 30000sec after initiating event. Moreover, in case of vessel wall failure, the ejection of the lower plenum debris starts at the time of vessel failure, without any delay.

The mass of lower plenum debris at the time of vessel breach is presented in Figure 5a in case of penetration modelling and Figure 5b in case without penetration modelling.



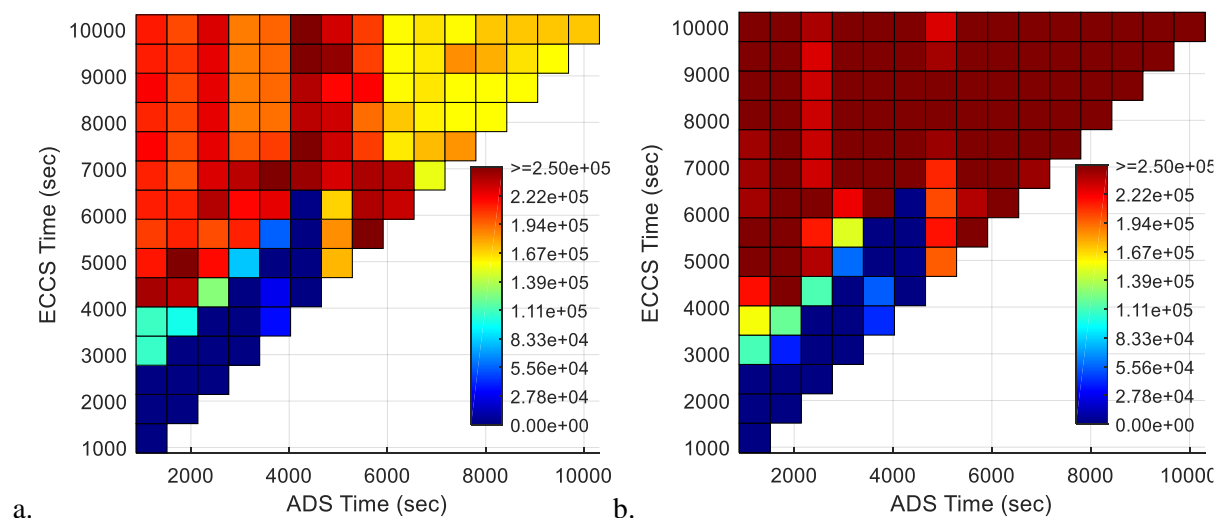a.                                                          b.

Figure 5. Expected value of the debris mass (kg) in LP at the time of vessel failure (a)with penetration modelling (b) without penetration modelling; as a function of ADS and ECCS Timing (sec)
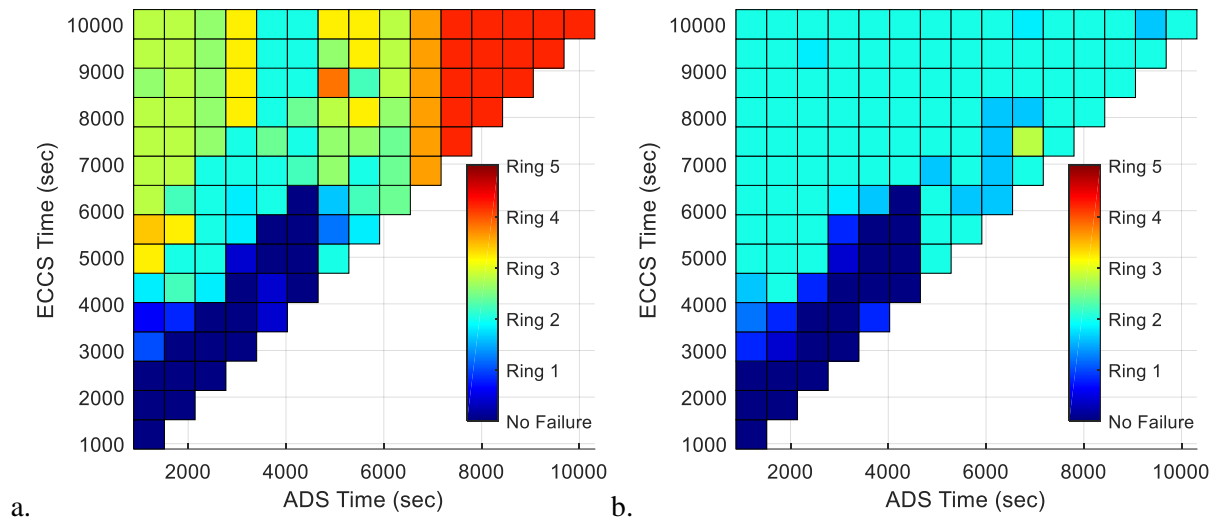
a.

b.

Figure 6. Expected Failure Location (Ring Number) (a) with penetration modelling (b) without penetration modelling; as a function of ADS and ECCS Timing (sec)

Figure 6a shows the expected location of penetration failure as a function of accident scenario, the results show that in the scenarios with ADS timing below 6000sec, penetration failure occurs in one of the central rings (most likely in the 2nd-3rd radial ring), while in the scenarios with ADS time above 6000 sec, penetration failure occurs in the 4th-5th radial rings. On the other hand, in the case without penetration modelling (see Figure 6b), vessel wall failure, in most of the cases, occurs in the 2nd ring, regardless of the accident scenario.

## 3.1.     Properties of the debris in LP

Figure 7a show the mass of molten metallic debris and Figure 7b shows the mass of molten oxidic debris at the time of vessel failure, with penetration modelling. The results show that the mass of molten metallic debris is significantly larger in scenarios with ADS timing below 4000sec, compared to the scenarios with ADS timing above 4000 sec (30-45tons vs. 10-15tons). The mass of molten oxidic debris is in the range of 0 to 7tons, without clear indication of the effect of accident scenario.
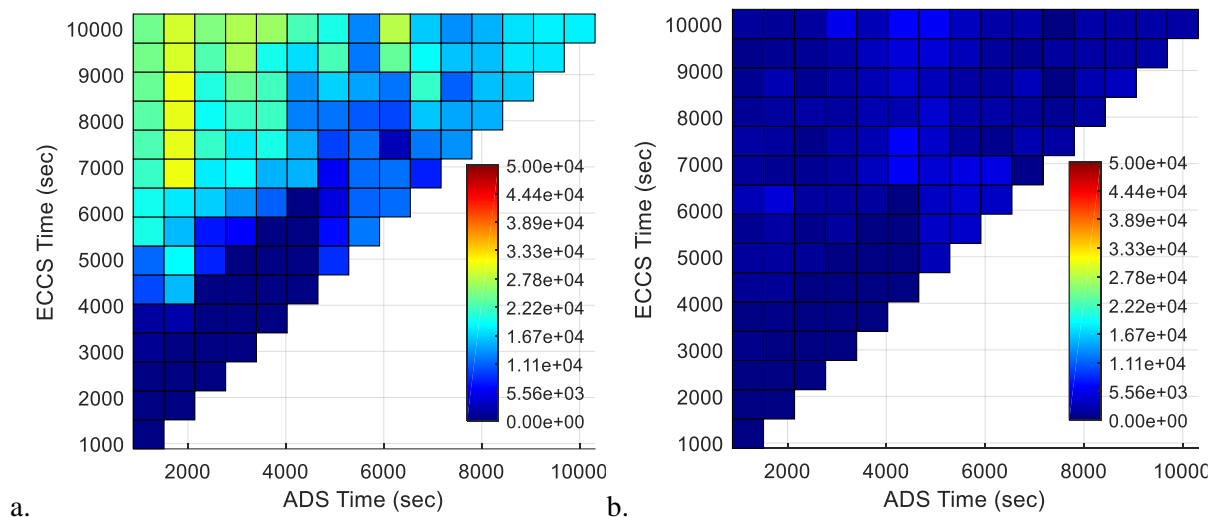


a.

b.

Figure 7. Expected value of (a) molten metallic debris mass (kg) (b) molten oxidic debris mass (kg), at the time of the release with penetration modelling; as a function of ADS and ECCS Timing (sec)

Figure 8 show the effect of accident scenario on the mass averaged superheat of the molten stainless steel debris in LP. The results suggest that in the scenarios with ADS timing below 6000sec, the mass

averaged superheat of stainless steel debris can reach 1000-1100K, while in scenarios with ADS timing above 6000sec it is in the rage of 300-500K.
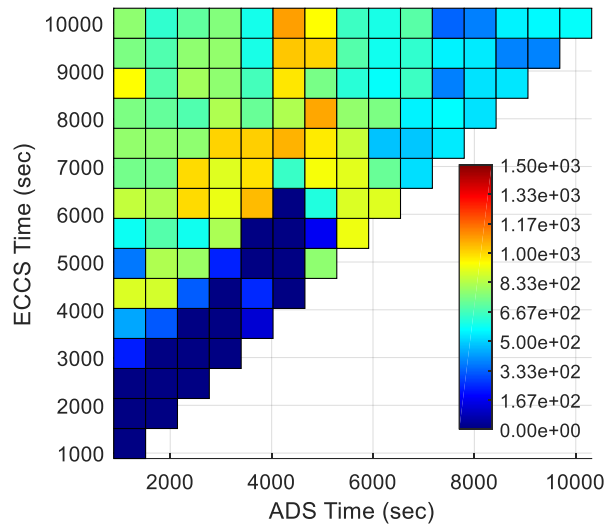


Figure 8. Expected value of LP molten stainless steel mass averaged superheat (K) at the time of the release with penetration modelling; as a function of ADS and ECCS Timing (sec)
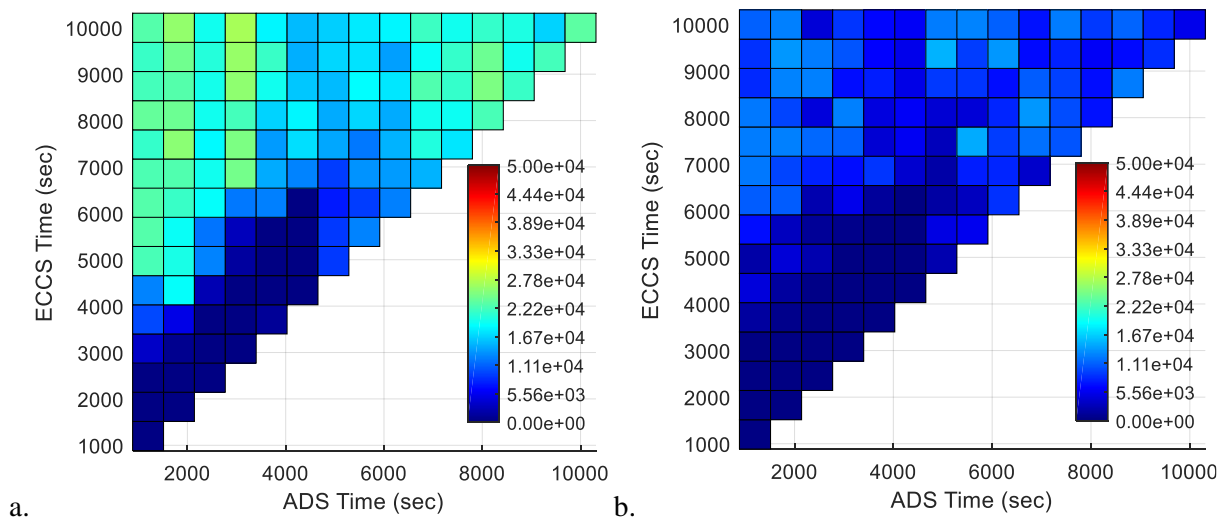


Figure 9. Expected value of (a) molten metallic debris mass (kg) (b) molten oxidic debris mass (kg), at the time of the release without penetration modelling; as a function of ADS and ECCS Timing (sec)

Figure 9a presents the mass of the molten metallic debris as a function of severe accident scenario, in the case of vessel wall failure without penetration modelling, the results show that the mass of molten metallic debris is in the range of 15-25 tons regardless of the accident scenario, with exception to the domain of scenarios with small relocated debris mass in the lower plenum see Figure 5. The mass of molten metallic debris at the time of vessel breach due to vessel wall failure (no penetration modelling) is significantly smaller compared to the scenarios with penetration modelling (see Figure 7a), even though the vessel breach in the case without penetration modelling occurs significantly later compared to the case with penetration modelling (e.g. 10000 to 20000 sec difference), and results in significantly larger values of the mass averaged superheat (see Figure 10, ~1200-1300K vs. ~1100K at most in case with penetration modelling, see Figure 8). This difference might be due to the effect of molten pool models in MELCOR code. It is assumed in MELCOR that particulate debris will sink into a molten pool, displacing the molten pool volume. Once solid debris components with lower melting point (such as stainless steel) start to melt, the volume occupied by solid debris decreases, the molten materials will occupy empty volume within the solid debris (reducing solid debris porosity). The remaining part will form a molten pool on top of the particulate debris, which will be displaced by the particulate debris

from the cell located above, which eventually can result in stainless steel-rich layer on top of the solid debris.

Figure 9b shows the mass of molten oxidic debris as a function of accident scenario, the results show that the mass of molten oxides ranges from approximately 7000 to over 10000kg in the whole scenario domain (with exception to the domain with small debris mass in LP).
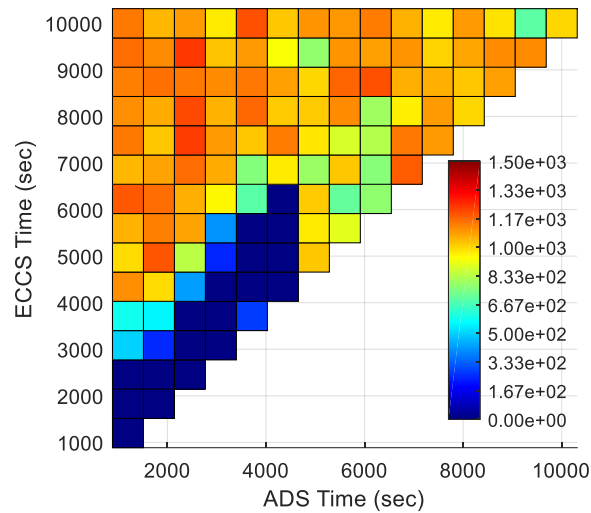


Figure 10. Expected value of Molten Stainless Steel in LP mass averaged superheat (K) at the time of the release without penetration modelling; as a function of ADS and ECCS Timing (sec)

### 3.2. Melt release from the vessel



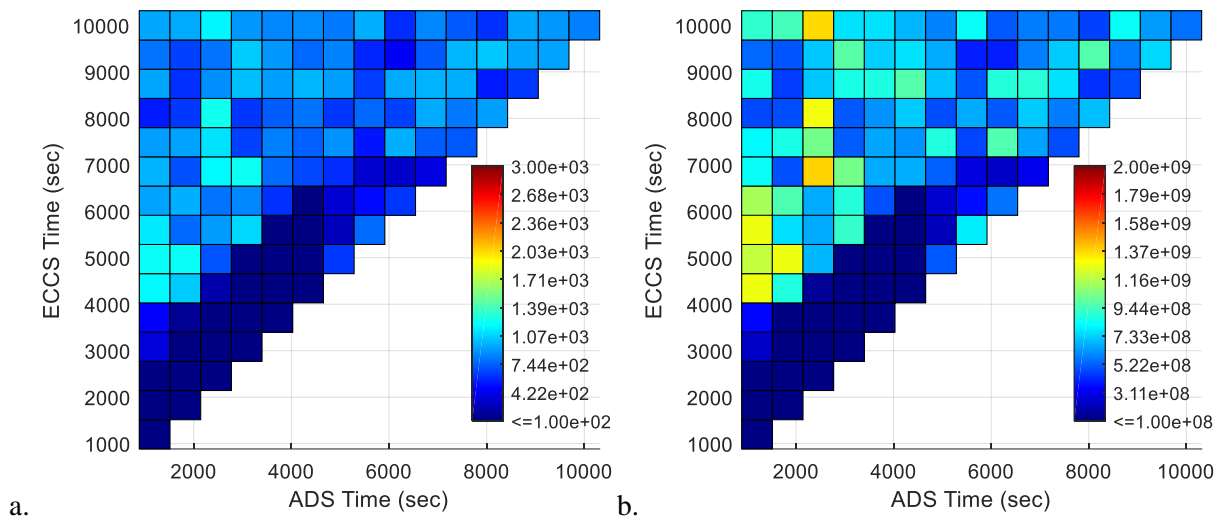a.                                                                 b.

Figure 11. Expected Value of (a) Maximum debris ejection rate (kg/s) (b) Maximum enthalpy rate (J/s) with penetration modelling, solid debris ejection ON (IDEJ=0); as a function of ADS and ECCS Timing (sec)

Figure 11a show the effect of accident scenarios on the expected value of the maximum debris ejection rate from the vessel, in the case of penetration modelling with solid debris ejection (IDEJ = 0). The results show that the maximum debris ejection rate ranges from approximately 400kg/s, mostly in the domain of scenarios with ADS timing in the range of 4000-6000sec, up to approximately 1200kg/s, mostly in the scenarios with early depressurization (ADS time <3000sec) and late depressurization (ADS time > 8000sec). The rate of enthalpy release, presented in Figure 11b, show that it is highly correlated with the debris ejection rate, however, some minor deviations can occur, due to the debris composition in LP. In scenarios with early depressurization ADS time < 3000sec, the maximum rate of

enthalpy release range from approximately 1e9 to 1.5e9 (J/s), while in the rest of the scenario domain it stay below 1.0e9 (J/s).
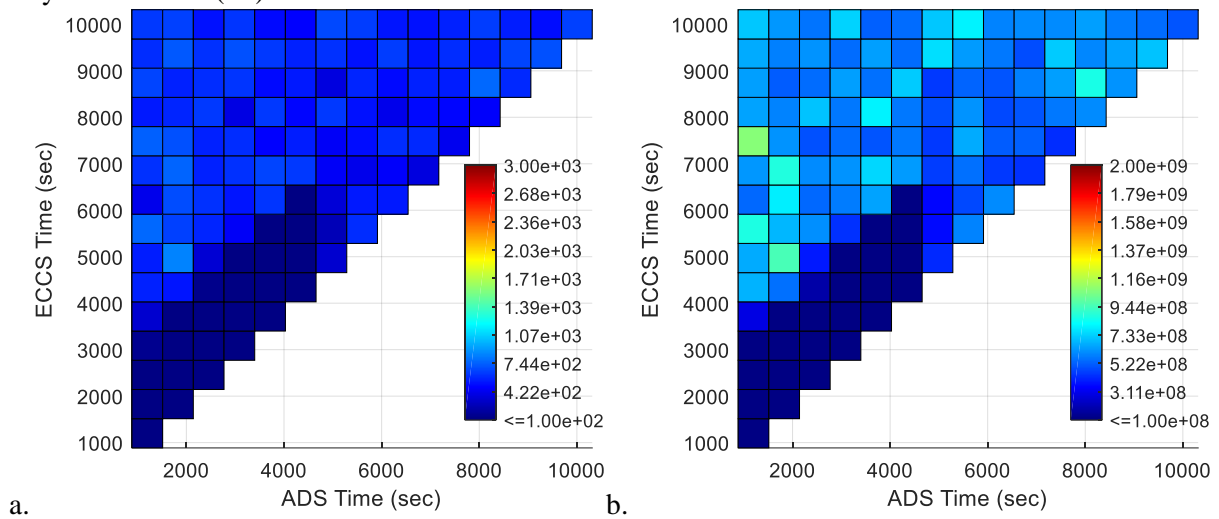


a.

b.

Figure 12. Expected Value of (a) Maximum debris ejection rate (kg/s) (b) Maximum enthalpy rate (J/s) with penetration modelling, solid debris ejection OFF (IDEJ=1); as a function of ADS and ECCS Timing (sec)
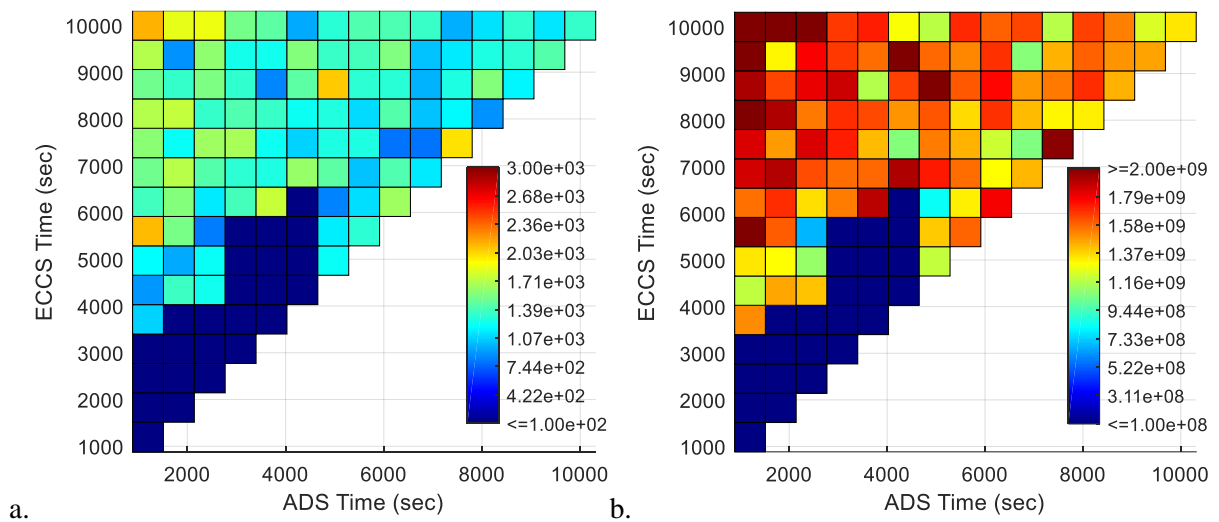


a.

b.

Figure 13. Expected Value of (a) Maximum debris ejection rate (kg/s) (b) Maximum enthalpy rate (J/s) without penetration modelling.; as a function of ADS and ECCS Timing (sec)

Figure 12a shows the debris ejection rate as a function of accident scenario in the case of vessel penetration modelling and with no solid debris ejection (IDEJ=1, see section 2 for details). The results show that the maximum debris ejection rate in case of IDEJ = 1 is significantly smaller (~400-500kg/s in most of the cases simulated) compared to IDEJ = 0 (see Figure 11a). This difference between the effect of solid debris ejection switch (IDEJ = 1 and IDEJ = 0) is also reflected in Figure 12b, where the maximum enthalpy release rate is approximately 5-8e8 (J/s), while in case of IDEJ=0 it is in the range of 8-15e8 (J/s).

Figure 13a illustrate the effect of accident scenarios on the maximum debris ejection rate and enthalpy release rate (Figure 13b) in case of vessel wall failure (without penetration modelling). The results show that the maximum values for the debris ejection rate can vary in the range from 2000-3000kg/s, regardless of accident scenario, since in case of gross failure of the vessel wall, it is assumed that all debris in the bottom axial level of the corresponding ring, regardless its state, is discharged linearly over 1s time step without taking into account failure opening diameter [6,7], this is also reflected in the values of enthalpy release rate, presented in the Figure 13b.

Note that in figures 11 and 13 (penetration failure with solid debris ejection on (IDEJ=0) and vessel wall failure), solid and liquid debris are ejected.

## 4. CONCLUSIONS

In this work we address the effect severe accident scenario and modeling options in MELCOR code on the processes of core degradation, relocation, vessel lower head failure and melt release in Nordic BWR. We show that severe accident scenario has a significant effect on the process of core degradation and relocation, debris properties in the lower head at the time of vessel failure, the vessel failure timing and melt release conditions. Furthermore, we have found that the effect of vessel failure modelling (i.e. with or without penetrations) and modelling of melt release (solid debris ejection mode) have dominant effect on the timing of vessel lower head failure and melt release mode.

### Acknowledgements

### References

1. Pavel Kudinov, Sergey Galushin, Dmitry Grishchenko, Sergey Yakush, Simone Basso, Alexander Konovalenko, Mikhail Davydov, "Application of Integrated Deterministic-Probabilistic Safety Analysis to Assessment of Severe Accident Management Effectiveness in Nordic BWRs," The 17th International Topical Meeting on Nuclear Reactor Thermal Hydraulics (NURETH-17) Paper: 21590, Qujiang Int'l Conference Center, Xi'an, China, September 3-8, 2017.
2. P. Kudinov, S. Galushin, W. Villanueva, S. Yakush, D. Grishenko, Development of Risk Oriented Approach for Assessment of Severe Accident Management Effectiveness in Nordic BWR, PSAM12, Hawaii, USA, June (2014).
3. D. Grishchenko, S. Galushin, S. Basso, P. Kudinov, "Application of TEXAS-V surrogate model to assessment of the containment failure risk due to steam explosion in a Nordic type BWR", *NUTHOS-11: The 11th International Topical Meeting on Nuclear Reactor Thermal Hydraulics, Operation and Safety*, Gyeongju, Korea, October 9-13, (2016).
4. Randall Gauntt, Donald Kalinich, Jeff Cardoni, Jesse Phillips, Andrew Goldmann, Susan Pickering, Matthew Francis, Kevin Robb, Larry Ott, Dean Wang, Curtis Smith, Shawn St.Germain, David Schwieder, Cherie Phelan, "Fukushima Daiichi Accident Study", SAND2012-6173, Sandia Report, SNL, (2012).
5. Lars Nilsson. "Development of an Input Model to MELCOR 1.8.5 for Oskarshamn 3 BWR", SKI Report, 2007:05, (2007).
6. L.L. Humphries, B.A. Beeny, F. Gelbard, D.L. Louie, J. Phillips, "MELCOR Computer Code Manuals", **Vol. 2**: Reference Manual Version 2.2.9541, SAND2017-0876 O, (2017).
7. L.L. Humphries, B.A. Beeny, F. Gelbard, D.L. Louie, J. Phillips, "MELCOR Computer Code Manuals", **Vol. 1**: Primer and Users' Guide Version 2.2.9541, SAND2017-0455 O, (2017).
8. Randall O. Gauntt, Nathan E. Bixler, and Kenneth C. Wagner, An Uncertainty Analysis of the Hydrogen Source Term for a Station Blackout Accident in Sequoyah Using MELCOR 1.8.5, SANDIA report, SAND2014-2210, March (2014).
9. Müller, C. Review of Debris Bed Cooling in TMI-2 Accident. Garching: GRS Forschungsinstitute, (2006).
10. Kudinov, P., Karbojian, A., Tran, C.-T., Villanueva, W., "Experimental Data on Fraction of Agglomerated Debris Obtained in the DEFOR-A Melt-Coolant Interaction Tests with High Melting Temperature Simulant Materials," Nuclear Engineering and Design, 263, October 2013, Pages 284-295, 10.1016/j.nucengdes.2013.06.011, 2013.
11. Magallon, D., "Characteristics of corium debris bed generated in large-scale fuel-coolant interaction experiments", *Nuclear Engineering and Design*, **236**, 2006, pp.1998–2009. (2006).

12. Kyle Ross, Jesse Phillips, Randall O. Gauntt, Kenneth C. Wagner, MELCOR Best Practices as Applied in the State-of-the-Art Reactor Consequence Analyses (SOARCA) Project, NUREG/CR-7008, (2014).

13. "Fukushima Daiichi Unit 1 Accident Progression Uncertainty Analysis and Implications for Decommissioning of Fukushima Reactors – Volume I", Sandia National Laboratories, SAND2016-0232, (2016).

14. S. Galushin, W. Villanueva, D. Grishchenko, P. Kudinov, "Development of core relocation surrogate model for prediction of debris properties in lower plenum of a Nordic BWR", *NUTHOS-11: The 11th International Topical Meeting on Nuclear Reactor Thermal Hydraulics, Operation and Safety*, Gyeongju, Korea, October 9-13, (2016).

15. Imtiaz K. Madni, Evaluation of MELCOR improvements: Peach Bottom Station Blackout Analyses, BNL-NUREG-49201. (1994).

16. A. Tuvelid, "Comparison of MELCOR and MAAP calculations of core relocation phenomena in Nordic BWR's" – Master Thesis, KTH, Stockholm, Sweden, (2016).

17. S. Galushin, P. Kudinov, "Comparison of MELCOR code versions predictions of the properties of relocated debris in lower plenum of Nordic BWR" 17th International Topical Meeting on Nuclear Reactor Thermal Hydraulics, Xi'an, Shaanxi, China, Sept. 3-8, (2017)

18. S. Galushin, P. Kudinov, "Effect of Severe Accident Scenario and Modeling Options in MELCOR on the Properties of Relocated Debris in Nordic BWR Lower Plenum", 17th International Topical Meeting on Nuclear Reactor Thermal Hydraulics, Xi'an, Shaanxi, China, Sept. 3-8, (2017).

19. S. Galushin, P. Kudinov, "Analysis of core degradation and relocation phenomena and scenarios in a Nordic-type BWR", *Nuclear Engineering and Design*, Volume **310**, Pages 125-141, ISSN 0029-5493, 15 December (2016).